

Orthogonalized Policy Optimization

Decoupling Sampling Geometry from Optimization Geometry in RLHF

Wang Zixian

China Mobile Communications Group Shandong Co., Ltd. Tai'an Branch

wangzixian@sd.chinamobile.com

Abstract

Recent alignment methods for large language models, including PPO, DPO, and IPO, are often presented as distinct algorithms. In this work, we show that many of these approaches implicitly conflate two fundamental and independent design choices: (i) the sampling geometry, which determines which samples dominate the gradient signal, and (ii) the optimization geometry, which determines how deviations in value are penalized.

We formalize this observation by expressing alignment as the minimization of a generalized distance between policy energy and target energy, parameterized by an α -divergence-based sampling weight and a Bregman divergence-based value metric. We demonstrate that the commonly used KL divergence induces an exponential penalty on unbounded value signals, leading to numerical instability and vanishing gradients in high-confidence regimes.

To address this issue, we propose **Orthogonalized Policy Optimization (OPO)**, a framework that explicitly decouples sampling geometry from optimization geometry. By combining α -weighted importance sampling with a χ^2 -induced quadratic regularization in ratio coordinates, OPO yields a simple and well-conditioned objective with linear gradient dynamics. This formulation maintains stable optimization while preserving peak-seeking behavior, and avoids gradient saturation even when model confidence is high. Our analysis positions OPO as a unifying perspective on existing alignment methods and provides a principled foundation for robust reasoning-oriented training.

1 Introduction

The field of Large Language Model (LLM) alignment has seen a proliferation of objective functions—PPO [2], DPO [1], IPO [7], GRPO [4]—each demonstrating effectiveness in specific settings. While these methods appear distinct, we observe that they share a common underlying structure that can be decomposed along two independent axes.

Observation: Implicit Conflation of Two Design Choices. We identify two fundamental degrees of freedom in alignment objectives:

1. **Sampling Geometry:** Which samples should dominate the gradient? This determines whether optimization is "average-case" (covering the target distribution) or "peak-seeking" (concentrating on high-reward modes).
2. **Optimization Geometry:** How should deviations in value be penalized? This determines the functional form of the gradient with respect to the policy's value signal.

In existing methods, these two choices are often coupled through a single divergence measure (typically KL). This implicit conflation can lead to undesirable interactions: for instance, adjusting the KL coefficient to control exploration simultaneously alters the curvature of the optimization landscape.

Diagnosis: The KL-Induced Exponential Penalty. The standard KL-regularized RL objective induces an exponential penalty on value signals via the log-sum-exp conjugate. While this is well-suited for probability distributions, the Advantage signal in RLHF is an unbounded real value. We show that this mismatch leads to:

- **Numerical Instability:** The exponential term can grow unboundedly.
- **Gradient Saturation:** In practice, KL-regularized preference objectives often reduce to sigmoid/logistic forms (e.g., DPO), which exhibit gradient saturation for large positive logit margins.

Contribution: Orthogonalized Policy Optimization (OPO). We propose **Orthogonalized Policy Optimization (OPO)**, a framework that explicitly decouples the two design axes. The key insight is to work in *ratio coordinates* rather than log-ratio coordinates, where the Pearson χ^2 divergence naturally induces a quadratic penalty. The OPO objective is:

$$\mathcal{L}_{\text{OPO}} = - \sum_{y \in S} \omega_\alpha(y) \cdot v_\theta(y) + \frac{\mu}{2} \sum_y v_\theta(y)^2, \quad v_\theta(y) = \frac{\pi_\theta(y)}{\pi_{\text{ref}}(y)} - 1 \quad (1)$$

where $\omega_\alpha(y)$ is an α -divergence-derived importance weight controlling sampling geometry, and $\frac{\mu}{2} v^2$ is the Pearson χ^2 -induced quadratic regularization controlling optimization geometry. Intuitively, ω_α increases the influence of rare high-quality samples while retaining a controllable interpolation to uniform weighting.

This decoupling allows independent control over "what to learn" (via α) and "how to penalize" (via μ), avoiding the entangled dynamics of KL-based methods. We show that this formulation yields a well-conditioned objective with a unique stable equilibrium and linear gradient dynamics.

2 Related Work

Preference Optimization and RLHF. Reinforcement Learning from Human Feedback (RLHF) typically involves learning a reward model from preferences and then optimizing a policy via PPO [2, 5, 6]. Direct Preference Optimization (DPO) [1] simplifies this by deriving a closed-form solution to the KL-constrained reward maximization problem. Recent variants extend this paradigm: IPO [7] adds a regularization term to prevent overfitting, SimPO [8] simplifies the reference-free objective.

f -Divergences in Machine Learning. The f -divergence family [9, 10] provides a unified framework for measuring distributional discrepancy. The Csiszár–Amari α -divergence [9, 11] continuously connects forward and reverse KL. Prior work has explored f -divergences in variational inference [12], GANs [13], and imitation learning [14]. In RL, α PPO [15] studied α -divergence as a trust-region constraint. Recently, APO [16] explored combining forward and reverse KL dynamics for standard preference optimization. OPO builds on these foundations by decomposing the divergence into independent geometry axes.

Trust-Region Methods. TRPO [3] enforces stability via explicit KL constraints, while PPO [2] approximates this with ratio clipping. ADPO [17] shows that anchored coordinates provide an implicit trust region via temperature-scaled curvature. OPO extends this by replacing the KL-based geometry with a quadratic (χ^2) geometry in ratio coordinates, providing a different form of implicit regularization.

3 Theoretical Framework: Two Independent Design Axes

We formalize the OPO framework by decomposing the alignment objective into two orthogonal components.

3.1 Coordinates: Ratio Space vs. Log-Ratio Space

Let the reference policy be π_{ref} . We define two coordinate systems for measuring policy deviation:

Definition 3.1 (Ratio Coordinates). The *density ratio* and *centered ratio* are:

$$t_\theta(y) := \frac{\pi_\theta(y)}{\pi_{\text{ref}}(y)}, \quad v_\theta(y) := t_\theta(y) - 1 = \frac{\pi_\theta(y)}{\pi_{\text{ref}}(y)} - 1 \quad (2)$$

Definition 3.2 (Log-Ratio Coordinates). The *log-ratio* (natural parameterization of LLMs) is:

$$\Delta_\theta(y) := \log \pi_\theta(y) - \log \pi_{\text{ref}}(y) \quad (3)$$

so that $t_\theta(y) = \exp(\Delta_\theta(y))$ and $v_\theta(y) = \exp(\Delta_\theta(y)) - 1$.

The key observation is that χ^2 divergence is naturally quadratic in ratio coordinates v , while KL divergence involves the log-ratio Δ . This distinction is crucial for understanding the gradient dynamics of different alignment objectives.

3.2 The Generalized Alignment Objective

We express the general alignment objective as:

$$\mathcal{L}(\theta) = \mathbb{E}_{y \sim \pi_{\text{sample}}} \left[w_\alpha(y) \cdot \mathcal{D}_\phi \left(\text{deviation}_\theta(y), \text{target}(y) \right) \right] \quad (4)$$

This formulation separates two independent design choices:

1. **Axis 1: Sampling Geometry (α)**: The weight $w_\alpha(y)$ determines how samples are weighted in the gradient.
2. **Axis 2: Optimization Geometry (ϕ)**: The distance \mathcal{D}_ϕ and the choice of deviation coordinates determine the penalty structure.

3.3 Axis 1: Sampling Geometry via α -Divergence

The weight $w_\alpha(y)$ controls the effective distribution from which the model learns. The parameter $\alpha \in [0, 1]$ interpolates between two regimes:

- $\alpha = 1$ (**Mode-Covering**): $w_\alpha(y) \approx 1$. All samples contribute equally. This corresponds to supervised fine-tuning (SFT) behavior.
- $\alpha \rightarrow 0$ (**Peak-Seeking**): This corresponds to peak-seeking behavior, often yielding exponentially amplified weights under standard RL formulations. High-reward samples dominate the gradient.

Most existing methods implicitly fix α . By treating it as an explicit parameter, we enable dynamic interpolation between coverage and exploitation.

3.4 Axis 2: Optimization Geometry via Divergence Choice

The choice of divergence determines the penalty structure. We compare two choices:

KL-Regularized Objectives (Exponential-Type Penalties). Under standard KL-regularized formulations, the dual induces exponential-type penalties in the log-ratio coordinate via the log-sum-exp operation:

- **Penalty term:** e^Δ .
- **Gradient scaling:** $\nabla \propto e^\Delta$.
- **Issue:** The gradient grows exponentially with Δ . In practice, KL-regularized preference objectives often reduce to sigmoid/logistic forms (e.g., DPO), which exhibit gradient saturation for large positive logit margins.

χ^2 Geometry (Quadratic Penalty in Ratio Coordinates). The Pearson χ^2 divergence naturally induces a quadratic penalty in ratio coordinates:

- **Penalty term:** $\frac{1}{2}v^2$.
- **Gradient scaling:** $\nabla \propto v$.
- **Advantage:** The gradient is linear in v , providing stable dynamics without saturation.

4 Orthogonalized Policy Optimization (OPO)

Combining the two axes with the χ^2 geometry in ratio coordinates, we obtain the OPO objective.

4.1 Pearson χ^2 Divergence: A Rigorous Foundation

We first establish the exact relationship between χ^2 divergence and quadratic penalties.

Proposition 4.1 (Pearson χ^2 induces a quadratic penalty in ratio coordinates). *Let $t(y) = \pi(y)/\pi_{\text{ref}}(y)$ and $v(y) = t(y) - 1$. The Pearson χ^2 divergence satisfies:*

$$D_{\chi^2}(\pi\|\pi_{\text{ref}}) = \frac{1}{2}\mathbb{E}_{y\sim\pi_{\text{ref}}}\left[(t(y) - 1)^2\right] = \frac{1}{2}\mathbb{E}_{\pi_{\text{ref}}}\left[v(y)^2\right] \quad (5)$$

Therefore, a χ^2 trust-region regularization yields a quadratic regularizer in the ratio coordinate v .

This is a definitional identity—the Pearson χ^2 divergence *is* the expected squared deviation of the density ratio from unity. This makes v the natural coordinate for χ^2 -regularized optimization.

4.2 OPO in Ratio Coordinates (Exact Form)

We define Orthogonalized Policy Optimization (OPO) by decoupling: (i) sampling geometry via α -weighted importance factors $\omega_\alpha(y)$, and (ii) optimization geometry via a Pearson χ^2 -motivated quadratic penalty in v_θ :

$$\boxed{\mathcal{L}_{\text{OPO}}^{\text{ratio}} = -\sum_{y\in S} \omega_\alpha(y) v_\theta(y) + \frac{\mu}{2}\mathbb{E}_{\pi_{\text{ref}}}\left[v_\theta(y)^2\right]} \quad (6)$$

where $v_\theta(y) = \pi_\theta(y)/\pi_{\text{ref}}(y) - 1$ is the centered ratio, and $\omega_\alpha(y)$ is an α -weighted importance factor. We adopt a generic α -divergence-inspired weighting scheme; one practical instantiation is $\omega_\alpha(y) = Q(y) \cdot [Q(y)/\tilde{p}_\theta(y)]^{1-\alpha}$, though other equivalent constructions are possible.

4.3 Log-Ratio Approximation for LLM Implementation

In practice, LLMs are parameterized in log-probability space, making it natural to work with the log-ratio $\Delta_\theta(y) = \log \pi_\theta(y) - \log \pi_{\text{ref}}(y)$. We establish the connection via Taylor expansion.

Corollary 4.2 (Local quadratic form in log-ratio space). *Let $\Delta_\theta(y) = \log \pi_\theta(y) - \log \pi_{\text{ref}}(y)$. Since $v_\theta(y) = \exp(\Delta_\theta(y)) - 1$, for $|\Delta_\theta(y)|$ sufficiently small (trust-region regime):*

$$v_\theta(y) = \Delta_\theta(y) + O(\Delta_\theta(y)^2), \quad v_\theta(y)^2 = \Delta_\theta(y)^2 + O(\Delta_\theta(y)^3) \quad (7)$$

Consequently, Equation (6) admits the practical approximation:

$$\boxed{\mathcal{L}_{\text{OPO}}^{\text{log}} \approx -\sum_{y\in S} \omega_\alpha(y) \Delta_\theta(y) + \frac{\mu}{2}\mathbb{E}_{\pi_{\text{ref}}}\left[\Delta_\theta(y)^2\right]} \quad (8)$$

which yields linear gradient dynamics in the log-ratio coordinate.

This approximation is valid when the policy remains close to the reference (the trust-region assumption underlying most RLHF methods). In practice, on-policy training with frequent reference updates ensures $|\Delta_\theta|$ remains small.

4.4 Gradient Dynamics

For the ratio-coordinate objective Equation (6), the gradient w.r.t. $v_\theta(y)$ is:

$$\nabla_v \mathcal{L}_{\text{OPO}}^{\text{ratio}} = -\omega_\alpha(y) + \mu v_\theta(y) \quad (9)$$

with the unique equilibrium:

$$v^*(y) = \frac{\omega_\alpha(y)}{\mu} \quad (10)$$

This linear relationship has several desirable properties:

1. **Stable Equilibrium:** The objective is strictly convex in $v_\theta(y)$ for fixed $\omega_\alpha(y)$, yielding a unique stationary point in the ratio coordinate.
2. **No Saturation:** Unlike sigmoid-based losses, the gradient magnitude does not vanish as v grows.
3. **Orthogonal Control:** Changing α (sampling) affects only ω_α ; changing μ (optimization) affects only the regularization strength. The two do not interact.

5 Theoretical Analysis

We now formalize the concept of orthogonality and analyze gradient behavior in high-confidence regimes.

5.1 Orthogonality of Design Axes

Definition 5.1 (Orthogonality of Design Axes). An alignment objective is *orthogonal* if the sampling geometry (parameterized by α) and the optimization geometry (parameterized by the divergence choice or μ) are decoupled: adjusting one does not implicitly alter the gradient structure determined by the other.

Non-Orthogonality in KL-Based Methods. In DPO and standard KL-regularized RLHF, the optimal policy has the form $\pi^* \propto \pi_{\text{ref}} \exp(r/\beta)$. This introduces \exp into both:

- The effective sample weight (via the importance ratio).
- The gradient penalty (via the softmax derivative).

Consequently, changing β (intended to control optimization aggressiveness) simultaneously alters the effective sample weighting. The two axes are entangled.

Orthogonality in OPO. In OPO (Equation (6)), the gradient is $\nabla = -\omega_\alpha + \mu v$. We observe:

- Changing α modifies ω_α but leaves the penalty structure (μv) unchanged.
- Changing μ modifies the regularization stiffness but leaves the importance weights (ω_α) unchanged.

This separation allows practitioners to independently tune "which samples matter" and "how strongly to regularize."

5.2 Gradient Behavior in High-Confidence Regimes

A key motivation for OPO is addressing the gradient vanishing issue in reasoning tasks.

The Saturation Problem in Sigmoid-Based Losses. In DPO and similar methods, the gradient is proportional to:

$$\nabla_{\text{DPO}} \propto \sigma(\Delta)(1 - \sigma(\Delta)) \quad (11)$$

where σ is the sigmoid function. As $\Delta \rightarrow \infty$ (high confidence), $\sigma(\Delta) \rightarrow 1$ and $\nabla \rightarrow 0$. This can cause optimization to stall even when further improvement is possible.

Non-Saturating Linear Drive in OPO. In OPO, the gradient is:

$$\nabla_{\text{OPO}} = -\omega_\alpha + \mu v \quad (12)$$

Even as v grows large, the gradient remains non-zero as long as $v < \omega_\alpha/\mu$. This provides a *non-saturating linear drive* toward the target, avoiding the saturation that plagues KL-based methods.

Remark 5.2 (Intuition). Informally, KL-based methods act like a "wall" that becomes harder and harder to push as confidence increases. OPO acts like a "spring" whose restoring force is proportional to displacement, providing consistent feedback throughout training.

6 Experiments

We conduct a preliminary empirical comparison between OPO and GSPO on mathematical reasoning tasks using the VERL framework.

6.1 Experimental Setup

Model and Data. We use Qwen3-1.7B as the base model and train on MATH Level 3 problems. Both methods use identical training configurations: 4 epochs, batch size 32, learning rate 2×10^{-6} , and 6 rollout generations per prompt.

Configurations.

- **OPO:** $\alpha = 0.6$, $\mu = 1.0$, adaptive τ with range $[0.2, 1.5]$.
- **GSPO:** Standard sentence-level GRPO with advantage normalization.

6.2 Results

Training Dynamics. Figure 1 shows the training accuracy (mean reward) over 224 training steps. Both methods exhibit similar convergence behavior, with OPO achieving slightly higher final accuracy (approximately 76% vs 71% averaged over the last 20 steps). The difference is modest but consistent across training.

Gradient Behavior. Figure 2 illustrates the gradient norm dynamics across training. OPO exhibits consistently higher gradient norms, suggesting more active optimization signal in accordance with the theoretical prediction of non-saturating linear gradients. The GSPO baseline shows lower and more stable gradient norms, potentially reflecting the implicit regularization from advantage normalization.

These preliminary results suggest that OPO achieves comparable or slightly better performance than GSPO on this task, while exhibiting gradient dynamics that align with theoretical predictions. Both methods converge stably without training instabilities. We emphasize that these experiments are preliminary and conducted on a single model scale.

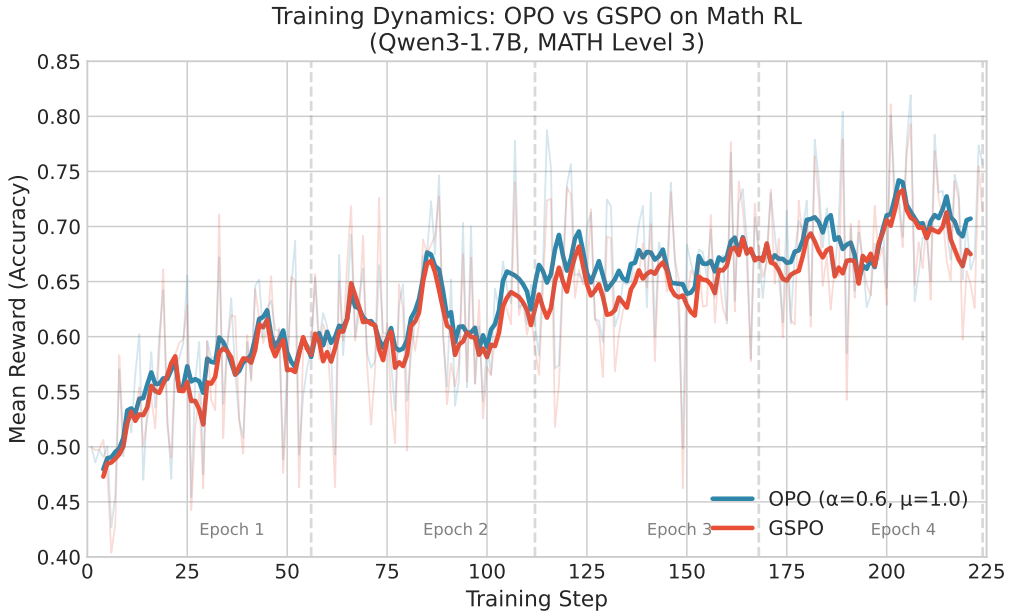


Figure 1: Training dynamics comparing OPO ($\alpha = 0.6, \mu = 1.0$) and GSPO on Qwen3-1.7B Math RL. Solid lines show 7-step moving averages; faded lines show raw values. Both methods achieve comparable final performance, with OPO showing a slight edge.

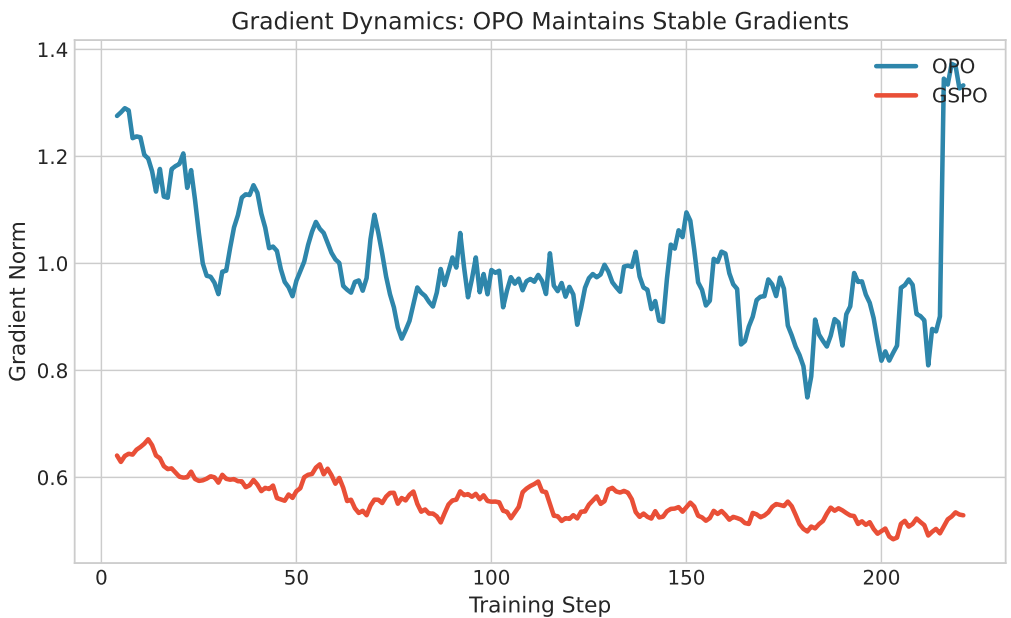


Figure 2: Gradient norm comparison. OPO maintains higher gradient norms throughout training, consistent with the theoretical prediction of non-saturating gradient dynamics.

7 Discussion

Relation to Existing Methods. OPO can be viewed as a generalization of existing alignment methods:

- Setting $\alpha = 1$ and removing the quadratic term recovers SFT-like behavior.
- Setting $\alpha \rightarrow 0$ and using KL geometry yields objectives with similar peak-seeking and exponential-type weighting effects as in KL-regularized preference optimization (e.g., DPO).
- OPO occupies the previously unexplored region of the design space: peak-seeking sampling with quadratic regularization in ratio coordinates.

Computational Cost. OPO incurs no additional model forward/backward passes compared to DPO/GRPO; the extra bookkeeping for ω_α is lightweight in practice.

Role of the Reference Policy. In OPO, the reference policy π_{ref} serves solely as an *origin* defining the coordinate system for the ratio $v_\theta = \pi_\theta / \pi_{\text{ref}} - 1$, rather than as an explicit regularizer via KL divergence. Stability is instead enforced by the quadratic penalty $\frac{\mu}{2}v^2$. This decoupling clarifies the distinct roles of anchoring (coordinate system) and regularization (optimization geometry).

Implementation Notes. The OPO objective (Equation (6)) involves expectations under π_{ref} . In practice:

- For on-policy training where samples come from $\pi_{\text{ref}} = \pi_{\text{old}}$, the batch itself provides an unbiased estimate.
- For off-policy settings, importance sampling or a separate reference sample set can be used.

Limitations. The framework introduces hyperparameters (α, μ) that may require tuning. Our experiments focus on reasoning tasks; validation on diverse domains (code generation, general instruction following) remains future work. Larger-scale experiments across diverse tasks and model sizes are needed to fully characterize the strengths and limitations of OPO.

8 Conclusion

We have presented **Orthogonalized Policy Optimization (OPO)**, a framework that decomposes alignment objectives into two independent design axes: sampling geometry and optimization geometry. By working in ratio coordinates where Pearson χ^2 divergence naturally induces quadratic penalties, OPO avoids the entangled dynamics of KL-based methods and provides a well-conditioned objective with linear gradient dynamics. Our analysis shows that OPO maintains stable optimization even in high-confidence regimes, addressing a key limitation of existing methods in reasoning tasks. We believe OPO provides a principled foundation for future work on robust and scalable LLM alignment.

References

- [1] R. Rafailov, A. Sharma, E. Mitchell, S. Ermon, C. D. Manning, and C. Finn. Direct Preference Optimization: Your Language Model is Secretly a Reward Model. *NeurIPS*, 2023.
- [2] J. Schulman, F. Wolski, P. Dhariwal, A. Radford, and O. Klimov. Proximal Policy Optimization Algorithms. arXiv:1707.06347, 2017.
- [3] J. Schulman, S. Levine, P. Moritz, M. I. Jordan, and P. Abbeel. Trust Region Policy Optimization. *ICML*, 2015.

- [4] Z. Shao, P. Wang, Q. Zhu, R. Xu, J. Song, X. Bi, H. Zhang, M. Zhang, Y. K. Li, Y. Wu, and D. Guo. DeepSeekMath: Pushing the Limits of Mathematical Reasoning in Open Language Models. arXiv:2402.03300, 2024.
- [5] P. Christiano, J. Leike, T. B. Brown, M. Martic, S. Legg, and D. Amodei. Deep Reinforcement Learning from Human Preferences. *NeurIPS*, 2017.
- [6] L. Ouyang, J. Wu, X. Jiang, D. Almeida, C. L. Wainwright, P. Mishkin, et al. Training Language Models to Follow Instructions with Human Feedback. *NeurIPS*, 2022.
- [7] M. G. Azar, M. Rowland, B. Piot, D. Guo, D. Calandriello, M. Valko, and R. Munos. A General Theoretical Paradigm to Understand Learning from Human Preferences. *AISTATS*, 2024.
- [8] Y. Meng, M. Xia, and D. Chen. SimPO: Simple Preference Optimization with a Reference-Free Reward. *NeurIPS*, 2024.
- [9] I. Csiszár. Information-type measures of difference of probability distributions and indirect observations. *Studia Sci. Math. Hungar.*, 2:299–318, 1967.
- [10] S. M. Ali and S. D. Silvey. A General Class of Coefficients of Divergence of One Distribution from Another. *JRSS-B*, 28(1):131–142, 1966.
- [11] S. Amari. *Information Geometry and Its Applications*. Springer, 2016.
- [12] Y. Li and R. E. Turner. Rényi Divergence Variational Inference. *NeurIPS*, 2016.
- [13] S. Nowozin, B. Cseke, and R. Tomioka. f-GAN: Training Generative Neural Samplers Using Variational Divergence Minimization. *NeurIPS*, 2016.
- [14] S. K. S. Ghasemipour, R. Zemel, and S. Gu. A Divergence Minimization Perspective on Imitation Learning Methods. *CoRL*, 2020.
- [15] H. Xu *et al.* Improving Proximal Policy Optimization with Alpha Divergence. *Neurocomputing*, 2023.
- [16] Z. Wang. APO: Alpha-Divergence Preference Optimization. arXiv:2512.22953, 2025.
- [17] Z. Wang. ADPO: Anchored Direct Preference Optimization. arXiv:2510.18913, 2025.